AIP | Applied Physics Letters

Optical modulation of terahertz behavior in silicon with structured surfaces

Xiaojun Wu, Xuecong Pan, Baogang Quan, and Li Wang

Citation: Applied Physics Letters **103**, 121112 (2013); doi: 10.1063/1.4821947
View online: http://dx.doi.org/10.1063/1.4821947
View Table of Contents: http://scitation.aip.org/content/aip/journal/apl/103/12?ver=pdfcov
Published by the AIP Publishing

Optical modulation of terahertz behavior in silicon with structured surfaces

Xiaojun Wu,[a] Xuecong Pan, Baogang Quan, and Li Wang
Beijing National Laboratory for Condensed Matter Physics, Institute of Physics, Chinese Academy of Sciences, Beijing 100190, China

(Received 1 July 2013; accepted 6 September 2013; published online 19 September 2013)

Optically modulated terahertz (THz) transmittance through Si with various resistivities, in particular the high-resistivity samples with a structured surface showing nanosized pillars or split-ring resonators (SRRs), was investigated. The samples with nanosized pillars display an increased transmittance and an accordingly reduced modulation depth. With SRRs on the surface, strongly selective modulation can be realized at the resonant frequencies where the transmittance is vanishingly small, whereas at the non-resonant frequencies, where the transmittance is large, the modulation depth is much greater. These results demonstrate an alternative route for the modulation of THz wave in the all-optical devices. © *2013 AIP Publishing LLC*.
[http://dx.doi.org/10.1063/1.4821947]

The unavailability of proper terahertz (THz) components, in particular for active THz devices, deters the development of THz-based techniques. In fact, it still has a long way to go before THz-based techniques such as those in communication can find large-scale implementation. THz devices that utilize electrically modulated liquid crystal have been demonstrated to be highly efficient,[1] they nevertheless show some quite intolerable deficiencies, for instance, slow response time. Recently, it was demonstrated that metamaterials can provide effective means for control and manipulation of THz waves,[2,3] via applying an electric field[4,5] or simply by temperature.[6,7] For instance, memory metamaterials on vanadium oxide substrate are sensitive to temperature variation, resulting in a shift of resonant frequencies,[5,6] while electrically gated metamaterials could be fabricated on thin layer of doped GaAs[4] or polymeric-supported graphene layers.[8] With all these designs, the THz devices bear some disadvantages when they are put into application or integration.

All-optical integration represents the development tendency for THz communication, for which optically manipulatable THz devices are highly demanded.[9,10] Optically controlled THz metamaterial devices are usually actualized by inserting laser-sensitive semiconductor materials such as Si in the gap region of the metastructures.[11] In this way, modulation of both intensity and phase of THz waves can be realized via photodoping in the semiconductor.[11,12] However, such optically active THz devices always require the input of high-energy femtosecond laser pulses with a slow repetition time, i.e., longer than the carrier lifetime in the semiconductor, in order to achieve a large modulation depth and/or a high sensitivity. Recently, an optically active THz filter of excellent flexibility has been proposed,[13] which is based on a mechanism referring to the light-induced free carrier absorption in semiconductors,[9] in which diffractive gratings for THz wave are produced in Si by a beam of white light. The light-induced patterns serve as a spatial light modulator so that some specific frequencies could be manipulated in a designed manner. The question is that it is not an easy task to improve the modulation depth simply by raising the light-induced THz absorption in Si.

In the current work, we report the optical modulation of THz behavior in Si wafers with a structured surface, i.e., with nanosized pillars or split-ring resonators (SRRs). It is found that both transmittance and modulation depth can be effectively modulated. Similar measurements by applying Si samples with nano-structured surfaces have not yet been reported. Selective modulation by SRRs will be understood with the aid of numerical simulation. These results may inspire further researches on the relevant problems concerning all-optical THz devices, especially for the Si nanostructures in THz technology.

The bulk Si samples here concerned include n-type Si (thickness 0.6 mm, resistivity 1–5 Ω·cm), p-type Si (thickness 0.6 mm, resistivity 7–13 Ω·cm), and n-type high resistivity (HR) Si (thickness 0.5 mm, resistivity 1000–2000 Ω·cm). In order to investigate the influence of surface morphology on the laser induced THz modulation, samples with a surface showing nanosized pillars, with or without an Au nanoparticle on the tip, were fabricated with HR Si wafer by using reactive ion etching. The etching conditions were chosen following Ref. 14, where self-assembled Au nanoparticles[15] were employed as mask for etching. The Au particles were removed thereafter by chemical etching using solution of I_2 (4g) + KI (2g) + doubly deionized water (500 ml). Typical SEM images of samples, of which the surface shows Si pillars with or without Au nanoparticles, are displayed in Fig. 1. Also SRRs were fabricated on a HR Si sample, the dimension of the SRR cell is specified in Fig. 1(c).[16] Comparative experiments were performed on a semi-insulating (100)-GaAs wafer (thickness 0.5 mm).

Experiment was conducted on a custom-designed angle-dependent THz time-domain spectroscopy system where both transmitted and reflected THz waves can be measured, see Fig. 1(d). The THz wave was generated from a low-temperature grown GaAs photoconductive antenna integrated with a Si hemisphere lens. A beam of p-polarized Ti: sapphire femtosecond laser (Maitai Spectra-Physics, repetition rate 80 MHz, pulse width 70 fs, central wavelength 800 nm, and averaged power 30 mW) was employed as the excitation

[a]Author to whom correspondence should be addressed. Electronic mail: wuxiaojun@aphy.iphy.ac.cn

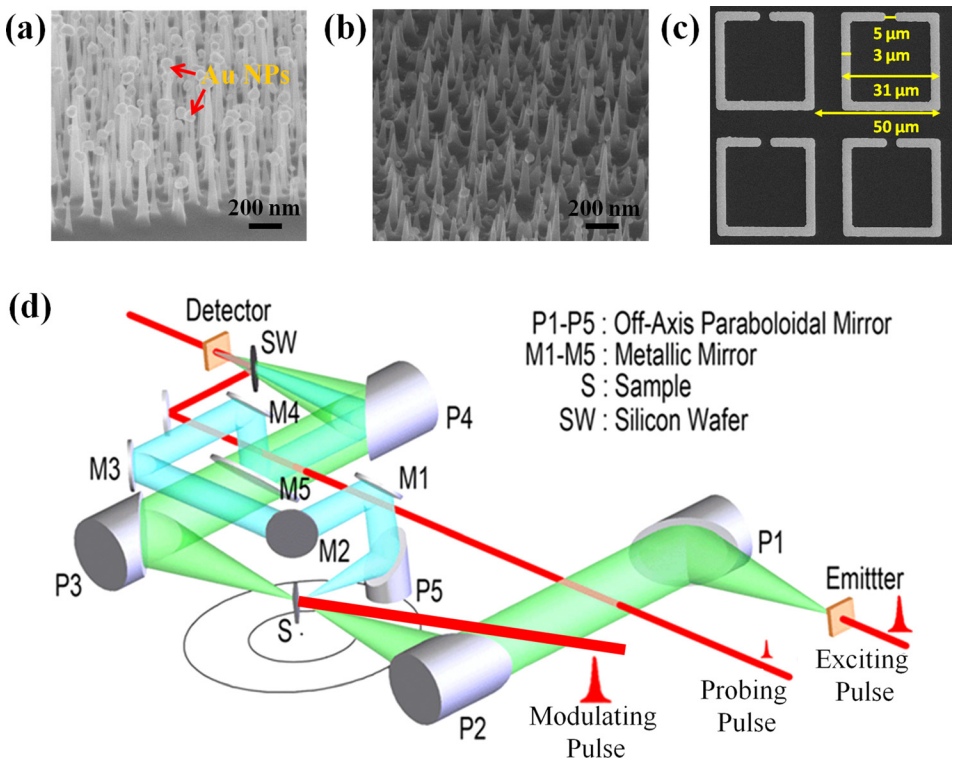

FIG. 1. SEM micrographs of the detected Si samples. (a) Bulk Si with a surface showing nanosized pillars, each with a gold particle on the tip. (b) The same sample as in (a), but with the gold particles almost completely removed; (c) SRRs fabricated on Si; (d) schematic sketch of the THz time-domain spectrometer which allows the measurement of both transmittance and reflectance.

source. THz detection was realized by using a ZnTe crystal via electro-optical sampling. The modulating beam was from the same laser as above, unfocused (spot diameter ~ 2.0 mm) and operating with a variable output power. The incident angle of the THz beam is fixed at 30°. The modulating beam strikes the samples almost along the normal direction. To verify the working mechanism for THz wave modulation, also a Ti:sapphire femtosecond laser operated with 5 kHz repetition rate and 100 fs pulse duration was used.

Fig. 2(a) plots the typical temporal waveforms of transmitted THz from a HR Si wafer illuminated by femtosecond laser pulses (repetition rate 80 MHz) with different modulating powers. The transmitted THz intensity decreases steadily with increasing the power of the modulating light. A slight phase shift towards shorter delay time was also observed in these waveforms. The corresponding Fourier spectra for the waveforms are presented in Fig. 2(b). Although the amplitude of the waveform decreases at increased modulating laser power, the Fourier spectral profiles for all the four measurements seem essentially conformal. It implies that a broadband modulation has been realized on HR Si via photodoping. In order to shed some light on the detailed modulation mechanism, the reflected THz signals from the same sample were also recorded. Fig. 2(c) shows the peak

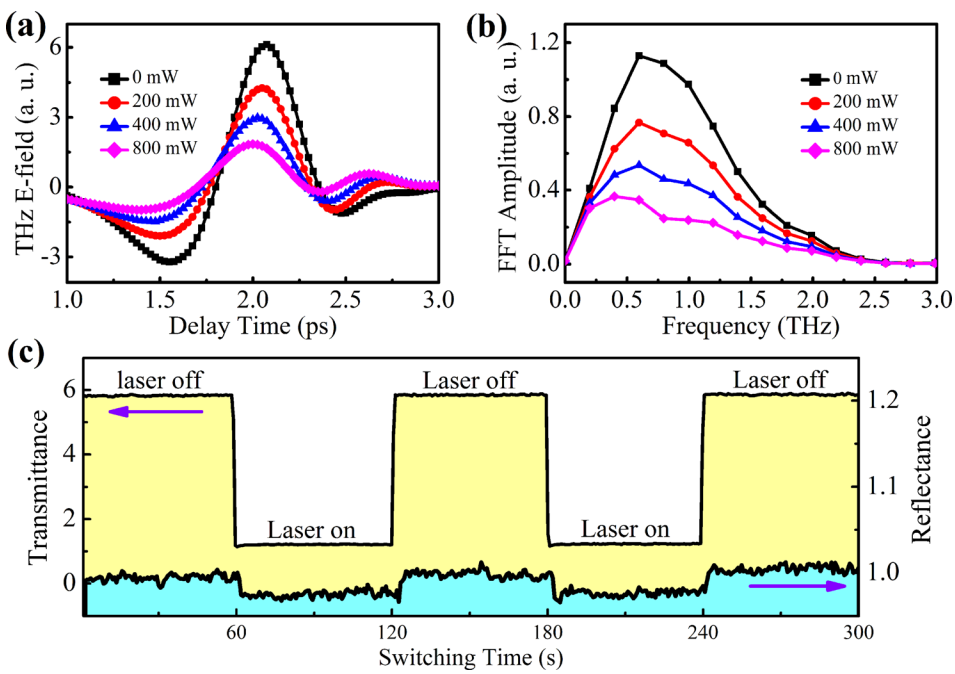

FIG. 2. Laser induced THz attenuation in transmittance and reflectance of high-resistivity bulk Si. (a) Typical THz temporal transmission waveforms and (b) their corresponding Fourier transformation spectra under different excitation power; (c) variation of THz transmittance and reflectance following the switching on/off of the modulating laser (800 mW).

amplitudes of both transmitted and reflected temporal waveforms for the case of an averaged modulating power of 800 mW. Both transmittance and reflectance decrease when the modulating laser is on. The modulation behavior is attributed to free carrier generation[17] from the time-averaged power transfer to the Si sample, although the transient operation of the pulsed modulating laser. The long lifetime of charged carriers ($\tau > 1\ \mu s$) in the lightly doped Si sample is in fact much longer than the pulse repetition time (12.5 ns) of the modulating laser. In order to further verify this point, the dynamical behavior of photodoping is determined by changing the temporal offset between the THz pulse and the modulation pulse. As expected, photodoping does not show any dependence on the choice of time delay. In addition, we replaced the HR Si by a semi-conducting GaAs, in which the lifetime of charge carriers is much less than 12.5 ns, and no detectable modulation behavior could be observed when the sample was subject to the same modulating laser referred to Fig. 2. If alternatively we replaced the modulating laser with a Ti:sapphire femtosecond laser (central wavelength 800 nm, repetition rate 5 kHz, pulse duration 100 fs), no considerable modulation was observed in HR Si either (not shown here). The pulse repetition time (0.2 ms) of the 5 kHz modulating laser is much shorter than the lifetime of charge carriers in the Si sample. These results point to the conclusion that it is the free carrier absorption that dominates the photodoping process.

Fig. 3(a) shows the peak-to-peak amplitude of temporal waveform for the transmitted THz signal as a function of modulating laser power. It can be seen that, for the three samples without any surface structure, the THz transmittance at all modulating powers is larger in samples of greater resistivity. The transmittance is further enhanced by the presence of Si pillars on the sample surface, and the residual Au particles on the pillar tips deterred to some extent such an enhanced transmittance. This is expected because the Au nanoparticles may act in some sense as a reflector for the modulating light. The fabrication process of the Si pillars may reduce the thickness of the Si sample and consequently inducing more THz transmission.

In contrast, the modulation depth, defined as $(T_0\text{-}T')/T_0$, where T_0 is the peak amplitude of THz waveform in the absence of modulating laser, while T' denotes the peak amplitude of THz waveform in the presence of modulating laser, shows an reversed tendency in these samples [Fig. 3(b)]. The sample with the lowest resistivity, i.e., the n-Si in Fig. 3(a),

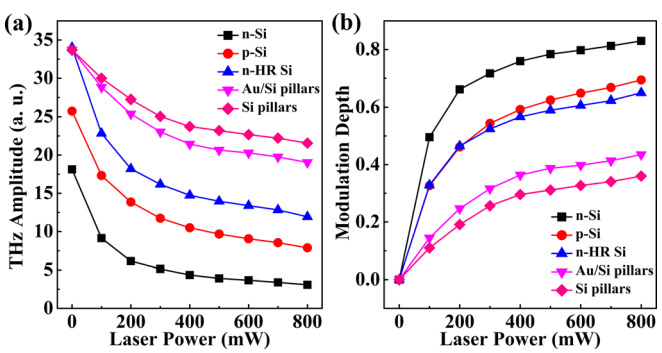

FIG. 3. (a) Transmitted THz peak-to-peak amplitude of the temporal waveforms, exemplified in Fig. 2, for a series of Si samples; and (b) the corresponding absolute modulation depth.

furnishes a maximum modulation depth of 83%, while for the sample with a surface showing purely nanosized pillars the maximum modulation depth is only 36%. Our original thought was to enhance the modulation depth of THz wave via exciting laser-induced surface plasmon resonance on the Si pillars with Au nanoparticles. Although it failed because of the difficulty for the satisfaction of phase matching, it implies that the modulation depth is highly correlated with the nature and surface condition of the Si samples, a merit that can be exploited for the design of THz devices for particular usages.

In order to realize intensity modulation for some particular frequencies in a frequency band, we explore the possibility of selective modulation by fabricating SRRs on the sample surface. Fig. 4(a) presents the transmission spectra of SRRs/Si under a modulating power of 0 mW, 400 mW, and 800 mW. It can be seen that the whole spectral profile continues to be lowered under increasing modulating power. At resonant frequencies, the transmittance is rarely influenced as the transmittance is already relatively low. But in the nonresonant portion, the modulation on the transmittance is quite obvious. These features become more accentuated in the view of the modulation depth, see Fig. 4(b). Under 800 mW, the averaged modulation depth in the frequency range from 0.5 to 1.0 THz amounts to as high as 65%. Figs. 4(c) and 4(d) show the mappings of the transmission and the modulation depth on the parametric plane subtended by THz frequency and the modulating power, which can help evaluate the effect of SRRs on the modulation behavior of the sample.

The mechanism for the selective modulation to the sample with SRRs can be better understood with the aid of full wave electromagnetic simulation of laser modulated THz transmission in sample.[16] The geometrical parameters of SRRs in the simulation are taken from the structures used in the current work [Fig. 1(c)]. Figs. 5(a) and 5(b) plot the THz transmission and the modulation depth given in pseudocolor on the parametric plane subtended by the frequency of THz wave and the imaginary part of the conductivity of the Si substrate, which is assumed to change from 0 S/m to 26 S/m when the modulating light is applied. The simulation results for both transmission and modulation depth agree well with the experimental observation. Figs. 5(c) and 5(d) show the electric field and the current density, respectively, for the cases of the imaginary part of conductivity being 0 S/m and 26 S/m. It can be seen that photodoping increases the free carrier density in Si substrate, resulting in a reduced electric field, and also a reduced current density, in the gap and at corners of the SRRs, which in turn brings down the transmission amplitude for resonant frequencies. As for the nonresonant portion, modulation is contributed from HR Si substrate. These results demonstrate the feasibility of selective modulation by light for some particular frequency bands by deliberate design of metamaterials, in conjunction with the free carrier absorption mechanism such as in Si.

The optically gated THz wave on Si, besides that it can be easily integrated into those devices for all-optical manipulation, has also some potential applications in THz time-domain spectroscopy.[16] HR Si wafers are usually employed in the THz time-domain spectrometer to reflect the probing laser pulse while let pass the incoming THz pulse. Laser induced free carrier absorption in HR Si will regulate the

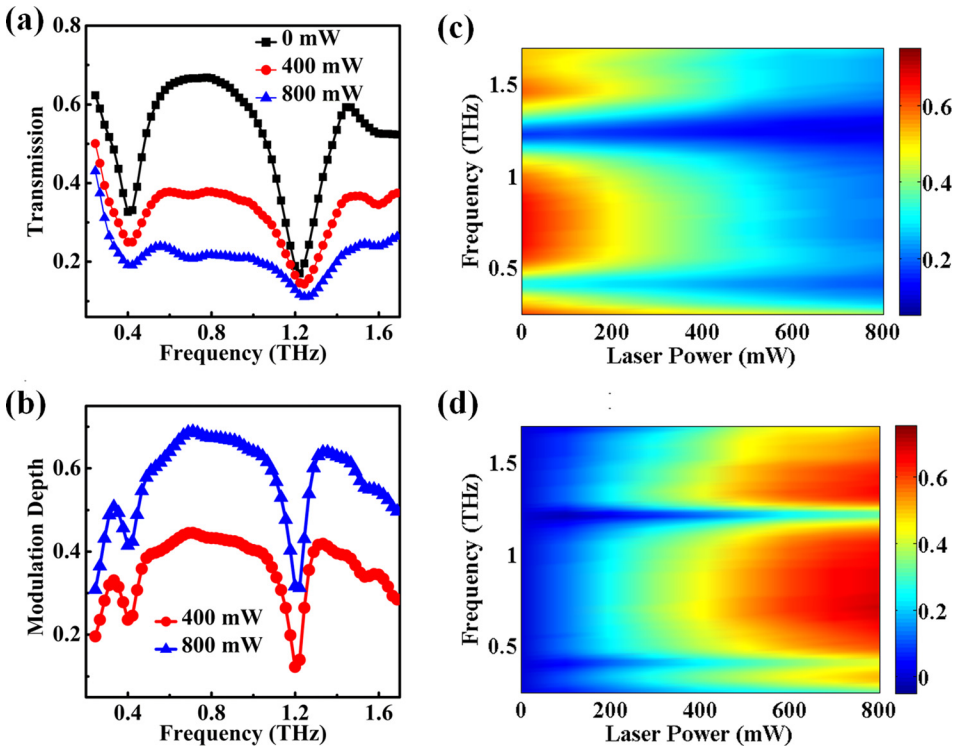

FIG. 4. Optical modulation of the THz behavior in high-resistivity Si with SRRs on surface. (a)–(b) Typical spectra of transmission and modulation depth. Power of modulating laser: 400 mW and 800 mW; (c) Mapping of the transmission and (d) that of modulation depth with regard to the power of modulating laser and the frequency of THz wave.

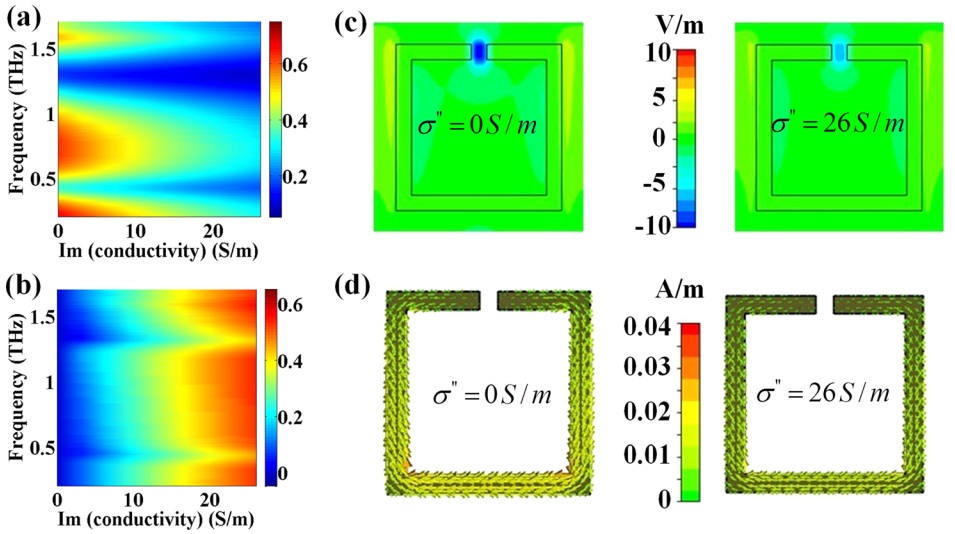

FIG. 5. Full wave electromagnetic simulation of laser modulated THz transmission in Si with SRRs on surface. (a) Transmission and (b) modulation depth in pseudocolor; (c) the electric field and (d) the current density for the cases of 0 and 26 S/m.

transmittance of THz wave if the repetition time of the probing laser pulse is shorter than the carriers' lifetime. Therefore, the detected THz signal differs to some extent from the original THz wave. By applying a HR Si with a structured surface such that for the THz wave to be tested the transmittance is high and modulation depth is low, which could raise the detection limit of THz time-domain spectroscopy. For the various applications in THz technique where a specific modulation depth is desired, for wideband or just for some particularly chosen frequencies, more meticulously designed structured surface for Si should be prepared.

In conclusion, we measured the laser-modulated THz transmittance of Si samples with various resistivities, in particular the high-resistivity samples having distinct surface features including nanosized pillars and SRRs structure. It was found that for the three samples with pristine surface, the sample with a high resistivity has the largest transmittance and the smallest modulation depth thereof. In comparison to the samples with a smooth surface, the high resistivity sample with a surface showing nanosized pillars displays an increased transmittance, and an accordingly reduced modulation depth. The Au nanoparticles on tips of the pillars bring down the transmittance of the sample, and the corresponding modulation length is raised a little. This work has paved the way by using nano-structured Si to all-optically manipulate THz wave and may inspire some related works in this research field. With SRRs on the surface, the HR Si displays strongly selective transmittance, thus at the resonant frequencies the transmittance is vanishingly small, whereas at the non-resonant frequencies the modulation depth can be significantly raised. The observations can be explained in the framework of laser induced free carrier absorption of THz

wave. This may provide an alternative route for the modulation of THz wave in some all-optical devices.

This work was supported by the National Natural Science Foundation of China under Grant Nos. 10834015 and 61077082.

[1]N. Vieweg, N. Born, I. AI-Naib, and M. Koch, J. Infrared Millim. Terahertz Waves **33**, 327 (2012).
[2]K. B. Fan, A. C. Strikwerda, X. Zhang, and R. D. Averitt, Phys. Rev. B **87**, 161104(R) (2013).
[3]J. B. Pendry, Nature **460**, 579 (2009).
[4]H. T. Chen, W. J. Padilla, J. M. Zide, A. C. Gossard, A. J. Taylor, and R. D. Averitt, Nature **444**, 597 (2006).
[5]Y.-G. Jeong, H. Bernien, J.-S. Kyoung, H.-R. Park, H.-S. Kim, J.-W. Choi, B.-J. Kim, H.-T. Kim, K. J. Ahn, and D.-S. Kim, Opt. Express **19**, 21211 (2011).
[6]T. Driscoll, H. T. Kim, B. G. Chae, B. J. Kim, Y. W. Lee, N. M. Jokerst, S. Palit, D. R. Smith, M. Di Ventra, and D. N. Basov, Science **325**, 1518 (2009).
[7]J. Gu, R. Singh, Z. Tian, W. Cao, Q. Xing, M. He, J. W. Zhang, J. Han, H.-T. Chen, and W. Zhang, Appl. Phys. Lett. **97**, 071102 (2010).
[8]S. H. Lee, M. Choi, T.-T. Kim, S. Lee, M. Liu, X. B. Yin, H. K. Choi, S. S. Lee, C.-G. Choi, X. Zhang, and B. Min, Nature Mater. **11**, 936 (2012).
[9]P. Weis, J. L. Garcia-Pomar, M. Höh, B. Reinhard, A. Brodyanski, and M. Rahm, ACS Nano **6**, 9118 (2012).
[10]M. Rahm, J.-S. Li, and W. J. Padilla, J. Infrared Millim. Terahertz Waves **34**, 1 (2013).
[11]H.-T. Chen, J. F. O'Hara, A. K. Azad, A. J. Taylor, R. D. Averitt, D. B. Shrekenhamer, and W. J. Padilla, Nat. Photonics **2**, 295 (2008).
[12]H.-T. Chen, W. J. Padilla, M. J. Cich, A. K. Azad, R. D. Averitt, and A. J. Taylor, Nat. Photonics **3**, 148 (2009).
[13]S. F. Busch, S. Schumann, C. Jansen, M. Scheller, M. Koch, and B. M. Fischer, Appl. Phys. Lett. **100**, 261109 (2012).
[14]Z. M. Xiao, J. C. She, S. Z. Deng, and N. S. Xu, J. Appl. Phys. **110**, 114323 (2011).
[15]R. H. Yao, J. C. She, N. S. Xu, S. Z. Deng, and J. Chen, J. Nanosci. Nanotechnol. **8**, 3487 (2008).
[16]X. J. Wu, B. G. Quan, X. C. Pan, X. L. Xu, X. C. Lu, C. Z. Gu, and L. Wang, Biosens. Bioelectron. **42**, 626 (2013).
[17]D. K. Schroder, R. N. Thomas, and J. C. Swartz, IEEE J. Solid-State Circuits **13**, 180 (1978).